

Brick Orientation Adjustment in the Automotive Industry using Image Processing Techniques

Charbel El Hachem
FEMTO-ST Institute, CNRS
Univ. Bourgogne Franche-Comté (UBFC)
Belfort, France
charbel.el_hachem@univ-fcomte.fr

Raoul Santiago
R&D center
Faurecia Clean Mobility
Bavans, France
raoul.santiago@faurecia.com

Loïc Painvin
R&D center
Faurecia Clean Mobility
Bavans, France
loic.painvin@faurecia.com

Gilles Perrot
FEMTO-ST Institute, CNRS
Univ. Bourgogne Franche-Comté (UBFC)
Belfort, France
gilles.perrot@univ-fcomte.fr

Raphaël Couturier
FEMTO-ST Institute, CNRS
Univ. Bourgogne Franche-Comté (UBFC)
Belfort, France
raphael.couturier@univ-fcomte.fr

Abstract—A ceramic monolith risks breakage during production of the exhaust systems in the automotive industry. This is due to its position at a specific angle throughout the canning phase (stuffing technique). To overcome this problem, quality control needs to be automated on each brick. This control aims to adjust, if needed, the positioning of the brick before starting the production.

This paper applies image processing techniques following the Canny-Hough method and reaches more than 99% of good detection of straight lines within a tolerance of ± 5 degrees, as requested by the plant. Some vision parameters (gain, exposure time and aperture range), have been tested in order to have a better visibility of the reference part. Furthermore, a repeatability test is validated in this paper, allowing the algorithm to be deployed in the plant.

The dataset is accessible on the following link: <https://doi.org/10.5281/zenodo.5948822>

Index Terms—quality control, automotive industry, image processing, ceramic monoliths, industry 4.0

I. INTRODUCTION

Quality control, by definition, implies the testing of an output sample against specifications. In the monolith ceramic production, quality control has been applied for the distribution of particles at the level of the filter [1]. Its quality control covers the performance of soot combustion in ceramic monoliths [2] and particle filtration based on the theory of the packed bed of spherical particles [3].

Faurecia, a major actor in the automotive industry at an international level, is working on guaranteeing the quality of their productions in order to meet the requirements of the client. This quality control needs to be automated and implemented in an accurate and repeatable system. The automation algorithm's execution should be less than 0.8 seconds in order to interact promptly with the operator. The correct position of the ceramic needs to reach a 99% level of accuracy, as required by the plant

with a tolerance of ± 5 degrees.

In this paper, the approach is as follows:

- 1) Listing the related works to detect straight lines.
- 2) Diving into image processing techniques to detect straight lines.
- 3) Comparing between different image processing techniques, and validating the chosen technique with a repeatability test.

This paper is organized as follows. Section II introduces the problem statement in monolith ceramics. Section III presents an overview of the existing work done in the area of deep learning and image processing. In Section IV, the proposed image processing method for line detection is explained. In Sections V and VI, the implementation details and the analysis of the experimental results are presented. The last section gives our concluding remarks.

II. PROBLEM STATEMENT

A. Stuffing technique

Ceramic monoliths sit right in the center of exhaust pipes and transform dangerous gases from the engine into a harmless gas. These are born from the combination of precious metals such as Platinum, Palladium and Rhodium. An example of a ceramic monolith is represented in Figure 1.

At the canning stage of the product's lifecycle, a metal envelope is reassembled with a mat and a ceramic [4]. As represented in Figure 2, this grouping is done with the stuffing technique [5]: it consists in enfolding the ceramic monolith in the mat, and in applying pressure on it inside the tube (the metal envelope). After that, a welding connects the end cones to each end of the cylinder to finish assembling the can.

B. Risk of breakage

The orientation of the ceramic monoliths does not affect the filtration of engine exhaust gases, but depending on its angle it increases the risk of breakage during the production of the

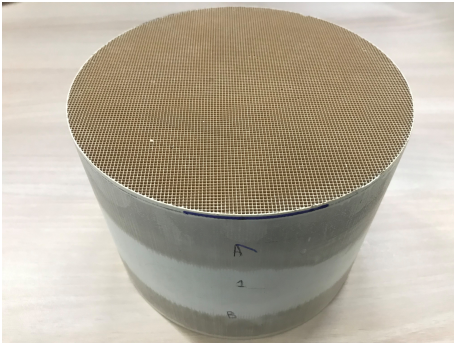


Fig. 1. Example of a ceramic monolith

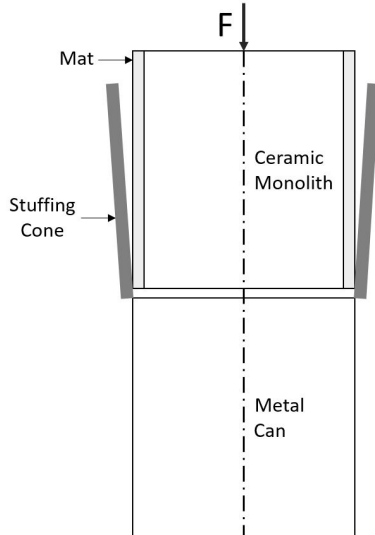


Fig. 2. Stuffing technique

exhaust systems: in particular, during the welding process that comes right after the stuffing technique.

This control aims to adjust, if needed, the orientation of the brick before starting the production. The ceramic monolith is positioned manually by the operator and a result of OK/NOT OK(NOK) should be displayed with no delay.

III. RELATED WORKS

Edges detection is achieved through two main approaches: image processing and deep learning [6]–[12].

A. Deep learning

Jiang *et al.* [13] have worked on detecting and classifying floral disease. The database includes images of the leaves of the affected plants. This classification is done using a neural network that requires 900 images per class and uses the Resnet-50 architecture. The results obtained reach a disease detection percentage equal to 98%.

The detection and classification of the causes of pulmonary diseases by means of X-ray images was carried out by Farooq *et al.* [14]. This classification makes it possible to differentiate between holy bodies and sick people (viral, bacteriological or

even Covid-19 risk). These data are divided into 4 classes and trained with Resnet50 architecture. The obtained model allows detection of 100% of Covid-19 contamination, 92% of viral contamination, and 95% of bacteriological contamination.

Many variants of traditional deep learning architectures appeared due to the efficiency of deep learning in classification tasks. Cheng *et al.* [15] have presented a new ResNet variant called ResGANet, able to classify medical images. The proposed architecture has 1.51-3.47 times fewer parameters than the original ResNet.

B. Image processing

Detection of retinal disease: diabetic retinopathy is highlighted by detecting the contour of the fundus [16]. This method transforms RGB images into grayscale images. The Canny edges approach will be applied to the latter in order to highlight the contours of the eyes and to detect the disease.

The detection of traffic lanes by means of a camera installed inside the vehicle was carried out by Rossi *et al.* [17]: Canny edges and Hough lines algorithms are applied to detect traffic lines. Subsequently, a Raspberry Pi controls the speed of the motor via an Arduino-uno.

The detection of bladder cancer by image processing using the Laplacian edges detector algorithm was carried out by Lorencin *et al.* [18]. This method allows areas of interest to be highlighted and achieves an accuracy of 99% on nearly 3000 images.

C. Decision-Making of the State-of-the-Art

After listing the state of the art, some parameters to take into consideration when making a decision such as the time for setup. For example, a deep learning solution can not be integrated in the plants conditions within one day, this is due to the number of images to be collected for the training. In addition, the training cannot be prepared in advance because lighting conditions are relative to the experimental environment. Due to the impact of deep learning on the time to market parameter, the image processing approach will be tested on this brick orientation adjustment.

As presented in the image processing state of the art, the methods to be tested to highlight edges are Canny edges and Laplacian edges detector.

IV. METHODS

In this section, two steps need to be differentiated: firstly, the highlighting of the edges and secondly the straight lines detection. The highlighting of the edges is a preparation step before the straight lines detection. The Canny and Laplacian will be tested for edges' highlighting, Hough transformation will be used for straight lines detection.

A. Highlighting edges

1) *Canny edges*: the Canny edge method allows to smooth an image and transform it into a binary image [19]. Two parameters are used to smooth an image: the minimum threshold and the maximum threshold allow to determine the desired

edge using the gradient formula.

When applying this image processing technique, a pixel belongs to the search edge if:

- 1) The pixel gradient is greater than the max threshold.
- 2) The pixel gradient is between the min threshold and the max threshold and is related to a pixel belonging to the edge.

A pixel does not belong to the search edge if:

- 1) The pixel gradient is below the minimum threshold.
- 2) The pixel gradient is between the min threshold and the max threshold and is not linked to a pixel belonging to the edge.

2) *Laplacian edges detector*: the Laplacian is a mathematical function that acts on each dimension of an image (x or y) [19]. It retrieves the evolution of the pixels of each dimension to apply a second derivative. The first derivative makes it possible to know the position of the most accentuated pixels and thus to be able to trace the contours of the images.

The second derivative has the same objective but also eliminates residual noises from the image. Once the function has been re-derived, the only points of interest are the points where the curve vanishes.

B. Hough lines

Hough lines allow to detect straight lines in an image. This detection is done either with the polar coordinate system or with the cartesian coordinate system. In this study, the OpenCV approach is applied and relies on the polar coordinate system [19].

In this function, a track of the intersection between the curves of every point in the image is kept. The threshold defines the number of intersections needed in order to declare it as a line. This line has θ and $r\theta$ as parameters of the intersection point. The impact of the methods listed above is represented in Figure 3.

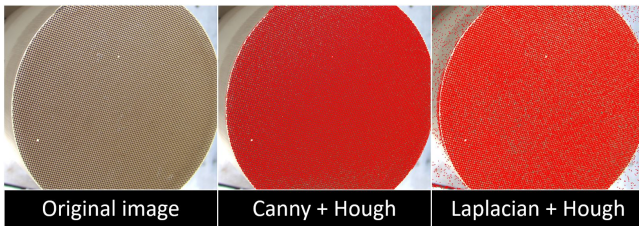


Fig. 3. Image processing methods applied on the ceramic monolith

C. Vision parameters

In order to fix the camera's configuration, many vision parameters have been tested to get a clear view of the brick channels [20]:

- 1) The gain parameter is the electronic amplification of the signal. A gain increase results in a more brightening image and negatively impact its quality. The value chosen during this project is 0.

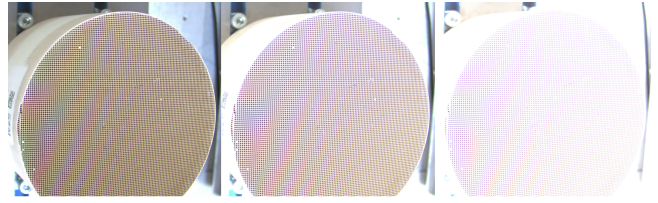


Fig. 4. Gain: minimum on the left, maximum on the right

- 2) The exposure time parameter is the time during which the sensor of the shooting device retrieves information from the image. It depends on the brightness and the aperture of the camera lens. If the exposure time is too low, the sensor cannot recover the pixel values and, as a result, the image is black. Conversely, if the exposure time is too high the image is white. For this project the exposure time is 0.478s.

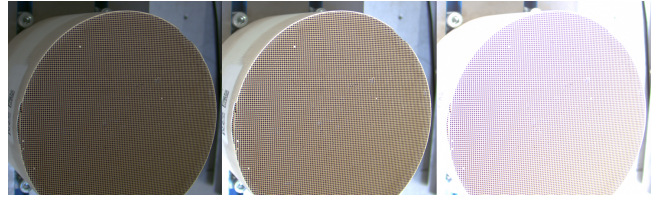


Fig. 5. Exposure time: minimum on the left, maximum on the right

- 3) The aperture range parameter is related to the size of the aperture of the camera's mount. The larger the opening is, the more information the sensor can collect. The value chosen for the aperture is the largest possible value, equal to f/4.



Fig. 6. Possible aperture values

These parameters have been adapted in order to reach the best visibility of the brick channels and applied on the collected images.

V. IMPLEMENTATION DETAILS

A. Experimental Environment

The experimental environment is powered by an Intel i5, 2.30 GHz processor with 64-bit on Windows 10 and 8 GB of RAM. The software programming environment is Python. As for the acquisition of images, a Basler acA2500-14gc camera equipped with a FUJINON HF8XA-5M C-mount has been installed (as shown in Figure 7). In the plant conditions, the canning machine has a cylinder above, this is why the camera is at 25 degrees from the vertical direction of the ceramic monolith in the realized tests.

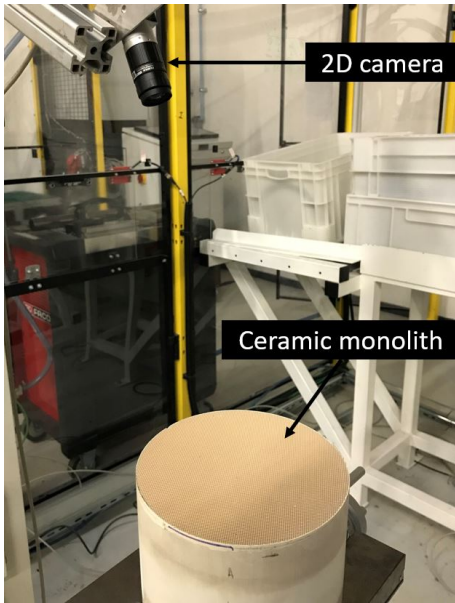


Fig. 7. Experimental environment: installation of the Basler camera

B. Angle Analysis

Thanks to the particular mesh of the brick, symmetry is obtained respectively with vertical and horizontal directions. These symmetries reduce the number of possible angles from $[0,360]$ to a range of $[0,90]$.

In this way, any angle greater than 90° is brought back to the interval $[0,90]$, for example an angle of 120° corresponds to an angle of 30° .

The tolerance defined by the plant is ± 5 degrees. Therefore, the calculated angle has to be in the range $[\text{real angle} - 5, \text{real angle} + 5]$.

C. Images collection

The images were collected as in the environment of Figure 7. The algorithm automatically collects images of the ceramic monolith with the fixed camera. Since the tolerance is ± 5 degrees, a step of 5 degrees is applied on a range from 0 to 90 degrees. Thereby, both methods (Hough and Laplacian) are tested on different angles.

VI. EXPERIMENTAL RESULTS

A. Coefficient of Determination

R-squared (R^2), called coefficient of determination, is a way of measuring how well the regression line approximates the actual data. It is an important indicator of how well the model will interact with future outcomes.

The results of Figure 8 show that:

- 1) 83% of the predicted angle values with Laplacian + Hough method fit with the real angle values.
- 2) 99.7% of the predicted angle values with Canny + Hough method fit with the real angle values.

Thereby, the Canny + Hough method bypasses the accuracy required by the plant (99%) with a tolerance of ± 5 degrees.

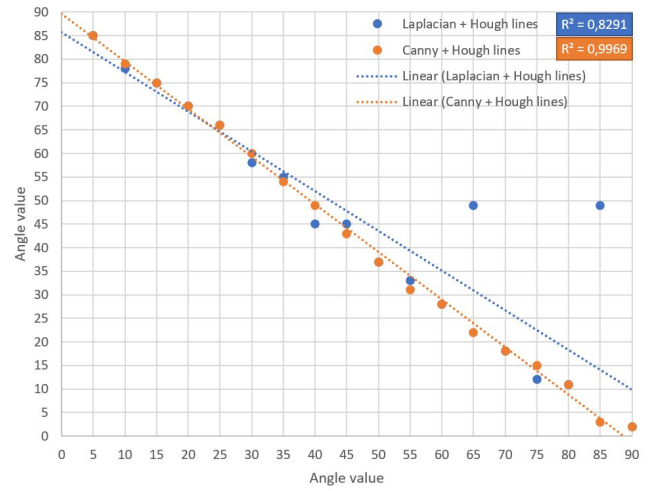


Fig. 8. Results of Canny-Hough and Laplacian-Hough with linear regression

The algorithm execution is 0.6 seconds per image. A repeatability test is applied on this method to validate its efficiency.

B. Repeatability test

In the repeatability test, the ceramic monolith is fixed and thousands of images are launched automatically to validate the accuracy of the algorithm through light changes. The first position is at 0 degree, while the last position is at 90 degrees. A step of 5 degrees is applied.

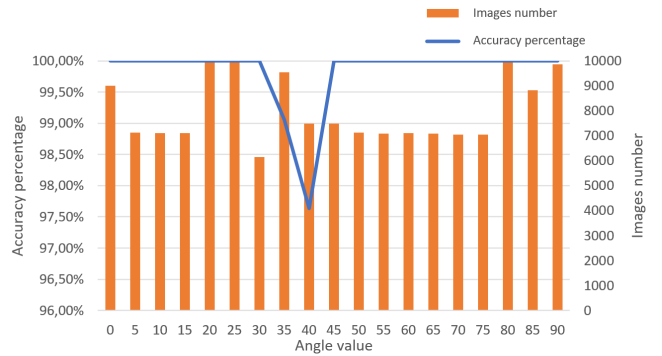


Fig. 9. Repeatability test validated with Canny-Hough method

The results of Figure 9 show that good detection has a percentage varying between 97.5% and 100% with an overall average of 99.826%. The algorithm execution of 0.6 seconds is also validated in this test. The Canny-Hough method is now ready to be deployed.

VII. CONCLUSION & FUTURE DIRECTIONS

Quality control being executed manually, remains not optimal. The automation of this control needs to be done via an algorithm deployed within a cell, offering complete autonomy to the factory.

In this contribution, the orientation of the ceramic is questioned and was solved with the method of image processing.

This method, previously applied for traffic lanes detection [17], has now been validated on the brick channels detection. The tests were carried out by applying a rotation of the ceramic by 5 degrees. The results show that with the Canny-Hough method, an accuracy of 99,826% is achieved within a tolerance of ± 5 degrees, as requested by the plant.

The proposed solution will be deployed in a Faurecia factory in order to validate the algorithm under real lighting conditions. This deployment will be carried out by the Digital Expertise & Development team, following a Human Machine Interface to be designed.

ACKNOWLEDGMENT

This work was done as a part of a CIFRE (N 2018/1029) project with Faurecia, funded by the Ministry of Higher Education and Research of France, managed by the Association Nationale de la Recherche et de la Technologie (ANRT) and was partially supported by the EIPHI Graduate School (contract "ANR-17-EURE0002").

The first author would like to thank Faurecia plant's staff for their availability.

REFERENCES

- [1] G Harvel, Jen-Shih Chang, D Ewing, Paul Fanson, and Masao Kakinohana. Measurement of multi-dimension soot distribution in diesel particulate filters by a dynamic neutron radiography. Technical report, SAE Technical Paper, 2009.
- [2] E Jiaqiang, Panyue Zheng, Dandan Han, Xiaohuan Zhao, and Yuanwang Deng. Effects analysis on soot combustion performance enhancement in a rotary diesel particulate filter unit during continuous microwave heating. *Fuel*, 276:118043, 2020.
- [3] Pi-qiang Tan, De-yuan Wang, Chao-jie Yao, Lei Zhu, Yin-huan Wang, Meng-hua Wang, Zhi-yuan Hu, and Di-ming Lou. Extended filtration model for diesel particulate filter based on diesel particulate matter morphology characteristics. *Fuel*, 277:118150, 2020.
- [4] Swapnil Shinde. Calibrated catalytic converter.
- [5] Sivanandi Rajadurai, Mauro K Tagomori, Jacob Berryhill, Anjum Baig, and Benny J Snider. Single seam stuffed converter design for thinwall substrates. Technical report, SAE Technical Paper, 1999.
- [6] Sen Jia, Shuguo Jiang, Zhijie Lin, Nanying Li, Meng Xu, and Shiqi Yu. A survey: Deep learning for hyperspectral image classification with few labeled samples. *Neurocomputing*, 448:179–204, 2021.
- [7] Devvi Sarwinda, Radifa Hilya Paradisa, Alhadi Bustamam, and Pinkie Anggia. Deep learning in image classification using residual network (resnet) variants for detection of colorectal cancer. *Procedia Computer Science*, 179:423–431, 2021.
- [8] Mohd Anul Haq, Gazi Rahaman, Prashant Baral, and Abhijit Ghosh. Deep learning based supervised image classification using uav images for forest areas classification. *Journal of the Indian Society of Remote Sensing*, 49(3):601–606, 2021.
- [9] Prateek Agrawal, Deepak Chaudhary, Vishu Madaan, Anatoliy Zabrovskiy, Radu Prodan, Dragi Kimovski, and Christian Timmerer. Automated bank cheque verification using image processing and deep learning methods. *Multimedia Tools and Applications*, 80(4):5319–5350, 2021.
- [10] Lawrence C Ngugi, Moataz Abelwahab, and Mohammed Abo-Zahhad. Recent advances in image processing techniques for automated leaf pest and disease recognition—a review. *Information processing in agriculture*, 8(1):27–51, 2021.
- [11] Yonggu Kim and Gjergj Dodbiba. A novel method for simultaneous evaluation of particle geometry by using image processing analysis. *Powder Technology*, 393:60–73, 2021.
- [12] Rayyan Manwar, Mohsin Zafar, and Qiuyun Xu. Signal and image processing in biomedical photoacoustic imaging: a review. *Optics*, 2(1):1–24, 2021.
- [13] Ding Jiang, Fudong Li, Yuequan Yang, and Song Yu. A tomato leaf diseases classification method based on deep learning. In *2020 Chinese Control And Decision Conference (CCDC)*, pages 1446–1450. IEEE, 2020.
- [14] Muhammad Farooq and Abdul Hafeez. Covid-resnet: A deep learning framework for screening of covid19 from radiographs. *arXiv preprint arXiv:2003.14395*, 2020.
- [15] Junlong Cheng, Shengwei Tian, Long Yu, Chengrui Gao, Xiaojing Kang, Xiang Ma, Weidong Wu, Shijia Liu, and Hongchun Lu. Resganet: Residual group attention network for medical image classification and segmentation. *Medical Image Analysis*, 76:102313, 2022.
- [16] Nishant Dandekar, Jayesh Kulkarni, Riddhi Raut, and Karishma Raut. Extracting features from the fundus image using canny edge detection method for predetection of diabetic retinopathy. *VIVA-Tech International Journal for Research and Innovation*, 1(4):1–6, 2021.
- [17] Alfa Rossi, Nadim Ahmed, Sultanus Salehin, Tashfique Hasnine Choudhury, and Golam Sarowar. Real-time lane detection and motion planning in raspberry pi and arduino for an autonomous vehicle prototype. *arXiv preprint arXiv:2009.09391*, 2020.
- [18] Ivan Lorencin, Nikola Anelić, Josip Španjol, and Zlatan Car. Using multi-layer perceptron with laplacian edge detector for bladder cancer diagnosis. *Artificial Intelligence in Medicine*, 102:101746, 2020.
- [19] OpenCV documentation. Opencv website: docs.opencv.org.
- [20] Wistiti photo documentation. Wistiti photo website: <https://www.wistitiphoto.com/>.